

## **INTEGRATED MODEL FOR THE HYDRO-MECHANICAL EFFECTS OF VEGETATION AGAINST SHALLOW LANDSLIDES**

**Alejandro González-Ollauri \*, Slobodan B. Mickovski**

School of Engineering & Built Environment, Glasgow Caledonian University,  
Glasgow, G4 0BA Scotland, UK

\* Corresponding author E.mail: alejandro.ollauri@gcu.ac.uk

### **Abstract**

Shallow landslides are instability events that lead to dramatic soil mass wasting in sloping areas and are commonly triggered by intense rainfall episodes. Vegetation may reduce the likelihood of slope failure through different hydro-mechanical mechanisms that take place at the soil-plant-atmosphere interface. However, while vegetation's mechanical contribution has been widely recognized, its hydrological effects have been poorly quantified. In addition, most of the existing models lack a holistic approach, require difficult to measure parameters or are commercially based, making them hardly transferable to land planners and other researchers.

In this paper an integrated, robust and reproducible model framework is proposed and evaluated with the aim of assessing the hydro-mechanical effects of different vegetation types on slope stability using easily measureable and quantifiable input parameters. The output shows that the model framework is able to simulate the hydro-mechanical effects of vegetation in a realistic manner and that it can be readily applied to any vegetation, soil and climate types. It also demonstrates that vegetation has positive hydro-mechanical effects against shallow landslides, where plant biomass and evapotranspiration play an important role.

**Keywords:** *Slope stability, vegetation, hydro-mechanical effects, integrated model, R*

### **Introduction**

Shallow landslides are instability events that lead to dramatic soil mass wasting in sloping areas, exposing the disturbed sites to further erosion (Walker & Shiels, 2013). A large number of landslides are triggered by intense rainfall episodes (Lim et al., 1996; Ekanayake and Phillips, 1999; Simon and Collison, 2002; Lu and Godt, 2013) that infiltrate into the soil profile changing its degree of saturation and diminishing the hydro-mechanical forces that keep the soil particles stable (Ekanayake and Phillips, 2002; Rahardjo et al., 2005).

Vegetation may have characteristics required to reduce the likelihood of slope failure (Pollen-Bankhead and Simon, 2010; Stokes et al., 2014) through different hydro-mechanical mechanisms that take place at the soil-plant-atmosphere interface (Fig. 1), all of which should be integrated within a slope stability analysis to account for the vegetation effects against shallow landslides.

However, although the hydro-mechanical effects of vegetation on slope stability have been extensively documented overtime (e.g. Wu et al., 1979; Norris et al., 2008; Stokes et al., 2014), some of the mechanisms are still poorly understood or quantified. For example, the mechanism by which the roots reinforce the soil at failure is not yet clear (Mao et al., 2014).

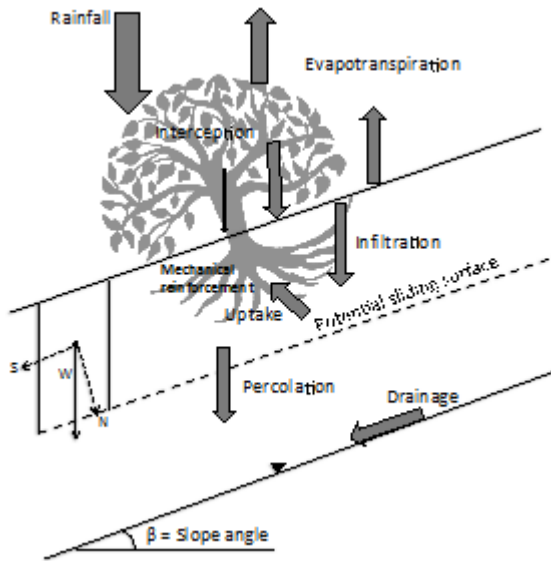


**Figure 1**

*Schematization of the hydro-mechanical mechanisms influenced by vegetation that affect slope stability and illustration of the forces used in limit equilibrium analysis: W: weight of the slope block; N: forces normal to the failure plane; S: forces along the failure plane. At equilibrium driving and resisting forces cancel each other*

On the other hand, the quantification of the hydrological effects of vegetation is difficult (Pollen-Bankhead & Simon, 2010) and severely lacking in the literature (Stokes et al., 2014). For the latter, the novel generalized effective stress principle and suction stress concept (Lu & Likos, 2004), and framework (Lu & Griffiths, 2004; Lu et al., 2010), can have a great potential for assessing the hydrological effects of vegetation on slope stability. To the best of our knowledge the effects of vegetation on soil strength has not yet been considered within this framework.

Additionally, most of the existing models for the effects of vegetation against shallow landslides just focus on a single process (e.g. root reinforcement), lacking a holistic view. Others are commercially based (e.g. GeoSlope), or are highly complex (e.g. 3-D FEM models), making their transferability to land planners and other researchers rather difficult. Therefore, it is desirable to implement simple, yet integrated, open source approaches that can be assessed with a few readily available input parameters, that include the essence of the main processes involved in a robust fashion; particularly attractive in resource limited situations.

In this paper an integrated, robust and reproducible systematic model framework is proposed and evaluated with the aim of assessing the hydro-mechanical effects of different vegetation types against shallow landslides using easy measurable and quantifiable input parameters. Firstly, in light of the effects of vegetation on slope stability a model approach and framework is proposed. Then, the different model

components are explained before setting a realistic unfavourable case scenario for running the model, illustrate its behaviour and gain insights into the potential effects of vegetation against shallow landslides.

## **Materials and Methods**

### **Model approach and framework**

The model approach (Fig. 2) considered a sloped soil-root continuum as the control volume (e.g. Jørgensen & Fath, 2011), with isotropic homogenous pedological properties, mechanically reinforced by vegetation roots and water table as its lower boundary. The forcing functions, represented by the infiltration of the net rainfall and the evapotranspiration, connect the control volume with the atmosphere and aboveground vegetation compartments. The forcing functions induce changes in the state variables, represented by the soil's inter-particle stress and the degree of saturation, which, in turn, directly affect the stability of the sloped control volume. Climatic, pedological and aboveground vegetation predictors determine the extent of the roots profile (see 2.3.5).

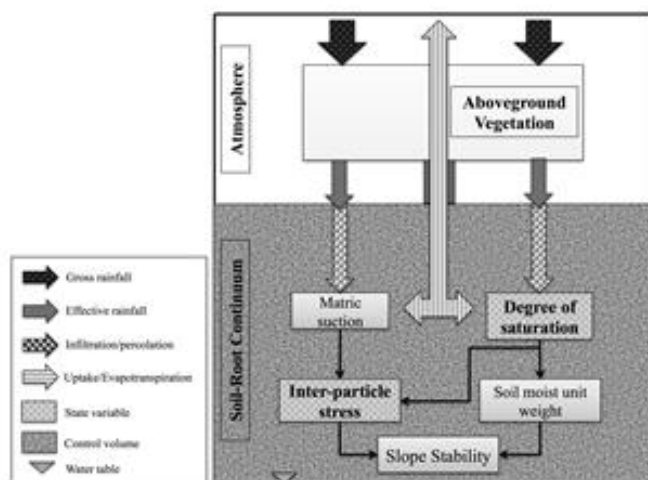


**Figure 2**  
*Conceptual model for the model approach where the soil-root continuum represents the control volume. Soil-Plant-Atmosphere compartments are connected through the forcing functions: infiltration of the net rainfall and evapotranspiration.*

The model framework comprised eight different sub-models: I = rainfall interception, II = infiltration, III = percolation, IV = evapotranspiration, V = root distribution, VI = plant uptake, VII = root reinforcement, VIII = suction stress. These converged into a final sub-model for slope stability analysis (IX). The different sub-models were configured in a cascade fashion and into two different paths depending on the hydro-biological process: wetting (i.e. I>II>III>VIII>IX) and drying (i.e. IV>V>VI>VIII>IX), respectively. A parallel path estimated the roots' mechanical reinforcement (i.e. V>VII>IX).

In addition, an independent model's module estimated the hydrological properties of the soil by means of pedotransfer functions (Rawls and Brakensiek, 1985; Saxton and Rawls, 2006).

The different sub-models were adapted and assembled in the open source code statistical software R 2.15.2 (R Core Team, 2012). The equations, parameters and assumptions for each sub-model are shown in Tables 1 to 4.

### Vegetation in slope stability analysis; core model

Slope stability analysis of rainfall-induced landslides can be carried out with the classical 1-D infinite slope approach due to their mode of failure (i.e. shallow, translational, parallel to the slope plane) (e.g. Godt et al., 2009). This approach, based on the Limit Equilibrium Method (LEM; Fig. 1) (e.g. Bishop, 1955), estimates a Factor of Safety (i.e. FoS; Eq. 2) as the ratio of the resisting forces and the driving forces (Fig. 1); whenever the driving forces overcome the resisting ones (i.e. FoS < 1) the slope is considered to have failed. The driving forces are depicted by the normal shear stresses ( $\sigma_N$ ) acting on the shear plane (i.e. the weight of the soil column ( $\gamma_s$ ; Eq. 3), subject to change with the degree of saturation ( $S_e$ ; Eq. 4), and the surcharge from the weight of the vegetation on the slope ( $W_v$ ; Eq. 5).

**Table 1.** Equations, parameters, source and assumptions for the slope stability, roots reinforcement and suction stress sub-models

Sub-model	Equations	Parameters	Source	Assumptions
Slope stability	$\tau = c' + (\sigma_N - \sigma^s) \tan \phi' \quad (2)$ $(1) \quad FS(z) = \frac{c' + c_R + ((\gamma_s(H_{wt} - z) + W_v) \cos^2 \beta - \sigma^s) \tan \phi'(z)}{(\gamma_s(H_{wt} - z) + W_v) \sin \beta \cos \beta}$ $\gamma_{soil} = \gamma_w \left( \frac{G_s + e S_e}{1 + e} \right) \quad (4)$ $S_e = \frac{\theta_n}{\theta_s} \quad (5)$ $W_v = M_v g \quad (3)$	<p>FoS: Factor of safety  <math>c'</math>: soil cohesion (kPa)  <math>c_R</math>: roots additional apparent cohesion (kPa)  <math>\gamma_s</math>: soil moist unit weight  <math>H_{wt}</math>: water table depth (m)  <math>z</math>: soil depth (m)  <math>W_v</math>: vegetation surcharge (kPa)  <math>\beta</math>: slope angle (radians)  <math>\phi'</math>: angle of internal friction (radians)  <math>\sigma^s</math>: suction stress (kPa)  <math>G_s</math>: specific gravity ( )  <math>e</math>: void ratio  <math>S_e</math>: degree of saturation  <math>\theta_n</math>: volumetric moisture content  <math>\theta_s</math>: saturated volumetric moisture content  <math>M_v</math>: aboveground and belowground vegetation mass  <math>r</math>: soil shear strength</p>	Lu & Godt (2008)	<ul style="list-style-type: none"> <li>- Infinite slope.</li> <li>- Isotropic soil.</li> <li>- Slope is at its limit equilibrium.</li> <li>- FoS &gt; 1; stable</li> <li>- FoS &lt; 1; unstable</li> <li>- Water table is the lower boundary</li> <li>- Hydrological steady-state conditions</li> <li>- Simplified approach for estimating the degree of saturation</li> </ul>
Roots reinforcement	$C_R(z) = 1.2KT_rRAR(z) \quad (6)$	<p><math>G_R</math>: roots apparent cohesion (kPa)  <math>K_c</math>: correction factor  <math>T_r</math>: root mean tensile strength (kPa)  <math>RAR</math>: root area ratio  <math>z</math>: soil depth (mm)</p>	Wu et al. (1979)	<ul style="list-style-type: none"> <li>- Roots perpendicular to the shear plane.</li> <li>- At failure all roots break</li> </ul>
Suction stress	$\text{if } u_a - u_w \leq 0$ $\sigma^s = -(u_a - u_w) \quad (7)$ $\text{if } u_a - u_w > 0$ $\sigma^s = - \frac{(u_a - u_w)}{(1 + (\alpha(u_a - u_w))^n)^{\frac{n-1}{n}}} \quad (8)$ $u_a - u_w = \frac{-1}{\alpha} \ln \left( \left( 1 + \frac{q}{K_s} \right) e^{-\gamma_w \alpha z} - \frac{q}{K_s} \right) \quad (9)$ $\theta(\varphi) = \theta_r + (\theta_s - \theta_r) \left( \frac{1}{1 + (\alpha(u_a - u_w))^n} \right)^{1-\frac{1}{n}} \quad (10)$	<p><math>\sigma^s</math>: suction stress (kPa)  <math>u_a</math>: pore air pressure (kPa)  <math>u_w</math>: pore water pressure (kPa)  <math>u_s</math>: matric suction (kPa)  <math>\alpha</math>: inverse of air entry pressure (kPa<sup>-1</sup>)  <math>\gamma_w</math>: unit weight of water ( )  <math>z</math>: soil depth (m)  <math>q</math>: infiltration or evaporation rate (m/h)  <math>K_s</math>: saturated hydraulic conductivity (m/h)  <math>\theta(\varphi)</math>: soil water characteristic curve  <math>\theta_r</math>: residual volumetric moisture content  <math>\theta_s</math>: saturated volumetric moisture content  <math>n</math>: pore size distribution parameter</p>	<p>Lu et al. (2010)                      Lu &amp; Griffiths (2004)                      van Genuchten (1980)</p>	<ul style="list-style-type: none"> <li>- Isotropic soil.</li> <li>- Steady-state infiltration and evaporation rates.</li> <li>- If <math>u_a - u_w &lt; 0</math>; saturated conditions.</li> <li>- Under saturated conditions <math>\sigma^s = 0</math></li> <li>- Hysteresis is neglected; i.e. <math>\alpha</math> and <math>n</math> are equal for the wetting and drying processes</li> </ul>

On the contrary, the resisting forces are commonly assessed with the Mohr-Coulomb failure criterion (Eq. 1), which estimates the soil shear strength ( $\tau$ ) as a function of its hydro-

mechanical conditions and makes possible to invoke the hydro-mechanical effects of vegetation on slope stability.

**Table 2.** Equations, parameters, source and assumptions for rainfall interception and infiltration sub-models

Sub-model	Equations	Parameters	Source	Assumptions
Rainfall interception	$P_t = a_1 P_g - b_1$ (11)	$P_t$ : gross rainfall (mm)	Gash (1979)	- Rainfall is considered to occur as a series of discrete events - Mean evaporation rate estimated as $E=0.4R$ - Troughfall and stemflow infiltrate into the soil
	$P_s = a_2 P_g - b_2$ (12)	$P_t$ : troughfall (mm)	Van Dijk & Bruijnzeel (2001)	
	$i = P_g - (P_t + P_s)$ (13)	$a_1$ : regression coeff.	Deguchi et al. (2006)	
	$c = 1 - e^{-kLAI}$ (14)	$b_1$ : regression coeff.		
	$E_c = \frac{E}{c}$ (15)	$a_2$ : coeff. quantity intercepted by canopy		
	$S_c = \frac{S}{c}$ (16)	$b_2$ : coeff. quantity retained in trunk		
	$P_g' = \left(\frac{R}{E_c}\right) S_c \ln(1 - E_c R)$ (17)	$i$ : interception loss (mm)		
		$c$ : canopy cover fraction		
		$LAI$ : leaf area index		
		$k$ : extinction coeff.		
Infiltration		$E_c$ : mean evap. rate from sat.canopy (mm/event)		
		$E$ : mean evap.rate (mm/event)		
		$P_s'$ : rain threshold for canopy saturation (mm)		
		$S$ : canopy storage capacity (mm)		
		$R$ : mean rainfall on saturated canopy (mm/event)		
		$P$ : rainfall rate (mm/h)	Mein & Larson (1973)	- Isotropic soil
		$t_r$ : rainfall duration (h)		- Moisture is uniformly distributed throughout soil profile.
		$t_p$ : ponding time (h)		- Steady rainfall
		$F(t_p)$ : cumulative infiltration at ponding time (mm)		- $\theta_r$ represents initial conditions
		$K_s$ : saturated hydraulic conductivity (mm/h)		- $\max(F(t))$ = gross rainfall per event
	$\phi_f$ : wetting front head (mm)		- wetting front saturates the soil behind	
	$\theta_s$ : volumetric saturated moisture content		- wetting front is at constant head	
	$\theta_r$ : volumetric residual moisture content		- if no ponding, all rainfall infiltrates	
	$z_f$ : wetting front depth (mm)		- Wetting front stops when rain ceases	
	$F(t)$ : cumulative infiltration at $t$ (mm)			
	$t$ : time at a given cumulative infiltration (h)			
	$q$ : infiltration rate (mm/h)			
	$F(t) = \text{seq}\{from = 0, to = t_r, P\}$ (21)			
	$t = t_p + \left(\frac{1}{K_s}\right) \left( F(t) - F(t_p) + \phi_f(\theta_s - \theta_r) \ln \left( \frac{\phi_f(\theta_s - \theta_r) + F(t_p)}{\phi_f(\theta_s - \theta_r) + F(t)} \right) \right)$ (22)			
	if $t < t_p$ $q = P$ (23)			
	if $t > t_p$ $q = K_s \left( 1 + \left( \frac{\phi_f(\theta_s - \theta_r)}{F(t)} \right) \right)$ (24)			

**Mechanical contribution; roots reinforcement sub-model.** Small vegetation roots mechanically reinforce the soil through the effect of a “root mat” that provides additional cohesion to the soil (Waldron, 1977) which can be included in the Mohr-Coulomb equation (i.e.  $c_R$ ) (Wu et al., 1979; Ekanayake and Phillips, 2002; Stokes et al., 2008).

Out of the available approaches for the quantification of  $c_R$ , the simple breakage perpendicular reinforcement model (Eq. 6) (Wu et al., 1979) was considered here as a good approach for the preliminary assessment of vegetation reinforcement due to its simplicity, reduced amount of input parameters (i.e. root area ratio; RAR and root tensile strength;  $T_r$ ) and observed realistic application (Mickovski et al., 2008). Essentially, it considers that the roots are growing perpendicularly to the shear plane and, at failure, all of them break. In addition, a correction factor ( $K'$ ) (Schwarz et al. 2010; Preti, 2013) was included to reduce the effects of likely overestimations of the utilized model (Mickovski et al., 2009).

**Hydrological contribution; suction stress sub-model.** The hydrological contribution of vegetation to slope stability can be considered with the inclusion of the generalized effective stress principle (Lu and Likos, 2004) into the Mohr-

Coulomb failure criterion. The generalized effective stress concept expands and extends the classical approaches of Terzaghi and Bishop, respectively, and allows the consideration of variably saturated conditions within the soil profile (Lu et al., 2010) through the incorporation of the suction stress variable ( $\sigma^s$ ) in the Mohr-Coulomb equation (Eqs. 7-8). Suction stress stands for all the soil's inter-particle forces and it depends on the degree of saturation ( $S_e$ ), matric suction ( $u_a-u_w$ ) and soil hydrological properties. It can be estimated in the lab through a standard direct shear test (Head and Epps, 2011; Lu and Godt, 2013), or through a validated closed-form equation (Eq. 8) (Lu et al. 2010) if the fitting parameters of the Soil Water Characteristic Curve (SWCC; Eq. 10; van Genuchten (1980)) are known (i.e.  $\alpha$  and  $n$ ). Furthermore, the suction stress can be also assessed with soil depth under steady-state conditions using an analytical solution of Darcy's law to estimate the matric suction (i.e.  $u_a-u_w$ ) (Lu and Griffiths, 2004). This analytical solution (Eq. 9) accounts for the water flux dynamics in the soil profile (i.e. infiltration or evapotranspiration), which, in turn, are affected by the vegetation at the soil-plant-atmosphere interface and hence permits to consider the hydrological contribution of vegetation to slope stability.

### **Complementary sub-models**

**Rainfall interception sub-model.** Reflecting reality, in our model aboveground vegetation intercepts rainfall (Eqs. 11-13) and splits it between throughfall ( $P_t$ ) and stemflow ( $P_s$ ) following a linear relationship with the gross rainfall as the unique predictor variable (i.e. Gash-model; Gash, 1979). The revised Gash-model (van Dijk and Bruijnzeel, 2001) also accounts for seasonal and species-specific differences through the consideration of the aboveground canopy configuration and gives better results than the original version (Deguchi et al., 2006, Muzylo et al., 2009). The modified Beer-Lambert equation (Pitman, 1989) is used for estimating the canopy configuration (i.e. canopy cover fraction ( $c$ ) (Eq. 14)); only the leaf area index (LAI) and the light extinction coefficient ( $k$ ) are required for this (Wolf et al., 1972; Bréda, 2003).

**Infiltration sub-model.** The net rainfall (i.e. Gross rainfall - interception loss) will eventually infiltrate into the soil profile and field evidence suggests that one-dimensional vertical flow occurs in many circumstances (Stokes et al., 2008; Godt et al., 2009; Lu & Godt, 2013), as the well-known modified Green & Ampt model (Mein & Larson, 1973) simulates (Fig. 3). Derived from Darcy's law, it assumes infiltration from a ponded surface down to an isotropic soil profile of uniform water content (Rawls et al., 1989). The infiltrating water is assumed to travel as a piston flow with a sharp division between the saturated soil above the wetting front and the dry soil below (Neitsch et al., 2011). Setting the initial moisture conditions and knowing the rainfall intensity ( $P_N$ ) and duration ( $t_r$ ), one can estimate how far the wetting front travels in the vertical direction ( $z_f$ ; Eq.20), how long it takes ( $t$ ; Eq. 22), what is the infiltration rate at that stage ( $q$ ; Eq.23-24) and how much water runs off or enters the soil profile.

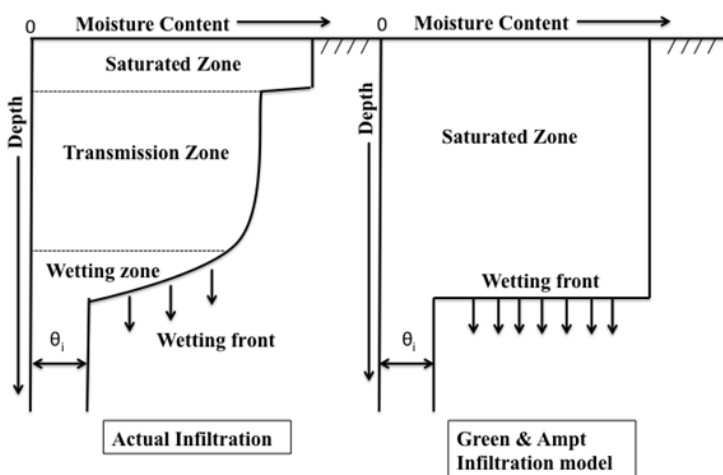


**Figure 3**  
Comparison of the moisture content distribution in the soil profile modelled by Green & Ampt and a typical observed distribution;  $\theta_i$ ; initial moisture content. (Neitsch et al., 2011).

Hence the degree of saturation in the soil profile after a rainfall episode can be also estimated if the soil hydrological properties are known; simple approximations can be made with pedotransfer functions (Eqs. 47-52) (Rawls and Brakensiek, 1985; Saxton and Rawls, 2006) that just require to know the soil texture, porosity (e.g. Head, 1980) and organic matter content (de Vos et al., 2005). The infiltration sub-model can be validated with the well-known ring infiltrometer test (Reynolds and Elrick, 1990).

**Percolation sub-model.** In the present framework it was assumed that the wetting front stops once the rain ceases. The excess water, relative to the field capacity, from the saturated wetting front would then percolate into the underlying unsaturated zone as a piston flow (Laio, 2006) and at a steady rate.

The percolation sub-model comprised simple mass balances to estimate the change in soil moisture content after percolation (Eqs. 25-28) and the approach suggested by Arnold et al. (1998) to estimate the percolation time ( $TT_{perc}$ ; Eq.29) and rate ( $q_{perc}$ ; Eq. 30), which uses a storage routing technique (Carter and Godfrey, 1960) and a known  $K_s$  (i.e. saturated hydraulic conductivity). The traveling distance ( $z_{perc}$ ; Eq.35) for the percolating water can be approximated through the hydraulic conductivity function (i.e. HCF; Eq. 34; e.g. Brooks and Corey, 1964) for a particular soil. Beyond the percolation depth hydrostatic conditions hold (i.e.  $q=0$ ) and the degree of saturation would be at its initial stage up to the lower boundary of the soil profile.

**Evapotranspiration sub-model.** Evapotranspiration is intimately related to plant water uptake (Jarvis, 1989), relying on the conditions at the soil-plant-atmosphere interface (Rodríguez-Iturbe and Porporato, 2004).

Priestly and Taylor (1972) proposed an equation (Eq. 36) based on Penman-Monteith's approach (Monteith, 1965) requiring few and easy measurable input parameters (i.e. mean air temperature, atmospheric pressure and solar radiation) to estimate the potential evapotranspiration rate for a given day of the year.

DOI: 10.6092/issn.2281-4485/4535

Additionally, the extension suggested by Savabi et al. (1989) was also used to allow the consideration of differences in the aboveground vegetation, distinguishing between below-canopy soil evaporation (Eq. 37) and plant transpiration (Eq. 38). However, the root profile distribution has to be known in order to assess to what extent evapotranspiration has an influence in the soil profile.

**Table 3.** Equations, parameters, source and assumptions for percolation and evapotranspiration (ETP) sub-models.

Sub-model	Equations	Parameters	Source	Assumptions
Percolation	$V_t = Z_f(t)A_{soil}$ (25)	$V_t$ : volume of saturated soil (m <sup>3</sup> )	Savabi & Williams (1989)	- Instantaneous percolation when rain stops
	$V_w = V_t \theta_s$ (26)	$Z(t)$ : wetting front depth (m)	Arnold et al. (1998)	- Preferential flow neglected
	$SW_{FC} = \theta_{FC} V_w$ (27)	$V_w$ : water volume in the saturated soil (m <sup>3</sup> )	Brooks & Corey (1964)	- Percolation as piston flow
	$SW_{ex} = (V_w - SW_{FC})$ (28)	$\theta_s$ : volumetric saturated moisture content		- Isotropic soil
	$TT_{perc} = \left( \frac{SW_{ex}}{K_s} \right)$ (29)	$\theta_{fc}$ : volumetric moisture content at field capacity		- Uniform moisture content in unsaturated soil
	$q_{perc} = (SW_{ex}) \left( 1 - \exp\left( \frac{-\Delta t}{TT_{perc}} \right) \right)$ (30)	$SW_{fc}$ : water at field capacity (mm)		- Excess water is all what exceeds field capacity
	$V_{unsat} = (z - z_{wf})A_{soil}$ (31)	$SW_{ex}$ : excess water in saturated soil (mm)		- All excess water percolates
	$SW_{unsat} = \theta_r V_{unsat}$ (32)	$TT_{perc}$ : travel time for percolation (h)		- Steady percolation rate
	$\theta_f = \frac{SW_f}{V_{unsat}}$ (33)	$K_s$ : saturated hydraulic conductivity (mm/h)		- Travel distance approximated with HCF at final moisture content
	$K(\theta) = K_s \left( \frac{\theta_s}{\theta_s} \right)^n$ (34)	$q_{perc}$ : percolation rate (mm/h)		- Beyond percolation front hydrostatic conditions hold
	$z_{perc} = K(\theta_f) TT_{perc}$ (35)	$\Delta t$ : time step for percolation (h)		
ETP	$Eu = 0.00128 \frac{R_{ni}}{58.3} \frac{\Delta}{\Delta + \gamma}$ (36)	$E_p$ : potential evapotranspiration rate (mm/day)	Priestley & Taylor (1972)	- $R_{ni}$ estimated following Allen et al. (1998)
	$E_{sp} = E_{we}^{-0.4LAI}$ (37)	$\Delta$ : Slope of saturation vapor pressure (kPa/°C)	Savabi & Williams (1989)	- 0.408R <sub>ni</sub> = mm/d
	$E_{tp} = \left( 1 - \left( \frac{E_{sp}}{E_u} \right) \right) E_u$ (38)	$\gamma$ : psychrometric constant (kPa/°C)		
	$d_x = 0.09 - 0.00077Cl + 0.000006Sa^2$ (39)	$R_{ni}$ : net solar radiation (MJ/m <sup>2</sup> day)		
		$LAI$ : leaf area index		
		$E_p$ : potential soil evaporation rate (mm/day)		
	$E_{tp}$ : potential plant transpiration rate (mm/day)			
	$d_e$ : maximum depth of evaporation from soil (m)			
	$Cf$ : percentage of clay content in soil (%)			
	$Sa$ : percentage of sand content in soil (%)			

**Root distribution sub-model.** The general behaviour of root density distribution with depth is rather simple, characterized by a decreasing trend (e.g. Gray & Baker, 2004; Mickovski et al., 2005; Mickovski et al., 2009; Preti et al., 2010). In fact, the vast majority of root profiles show exponential declines of root density with increasing depth (Schenk, 2008), which greatly depends on the climate and the soil types (Schenk and Jackson, 2002). Based on these facts, Laio et al. (2006) developed a very simple analytical approach for estimating the root profile as a function of easily determinable pedologic and climatic descriptors for water-controlled ecosystems (e.g. Rodríguez-Iturbe and Porporato, 2005). This approach, which has never been applied for temperate climates, was further extended and verified by Preti et al. (2010). It models the root cross-sectional area (Ar(z)) as an exponentially decreasing function of soil depth (Eq. 42) and the average rooting depth (*b*; Eq. 40). *b* is determined with readily available long-term climatic (e.g. UNEP; UK Met Office; BADC, Umweltdaten, etc.) and pedologic parameters. Ar(z) also depends on a scaling factor that is species-specific (Ar<sub>0</sub>; Eq. 41; Preti et al., 2010). The later can be easily determined through an allometric model (e.g.

Cheng & Niklas, 2007), requiring the characteristic aboveground biomass and the root mass density as input parameters. The outcome of this model can be used for estimating the root area ratio (RAR; Eq. 43) by dividing  $Ar(z)$  by the considered rooted soil area (Ars) and feed the roots reinforcement sub-model (see 2.2.1), or to estimate the root density distribution function ( $r(z)$ ; Eq. 44) and feed into the plant water uptake sub-model (see 2.3.6).

**Table 4.** Equations, parameters, source and assumptions for roots distribution and plant-water uptake sub-models, and pedotransfer functions.

Sub-model	Equations	Parameters	Source	Assumptions
Roots distribution	$b = \frac{\alpha'}{n(\theta_{FC} - \theta_{WP}) \left(1 - \left(\frac{\alpha' \lambda_p}{ETP}\right)\right)} \quad (40)$ $Ar_o = \frac{(M_a/\Omega)^{\frac{1}{\beta}}}{b \rho_r} \quad (41)$ $Az(z) = Ar_o e^{-\frac{z}{b}} \quad (42)$ $RAR(z) = \frac{Ar(z)}{Ars} \quad (43)$ $r(z) = \frac{Ar(z)}{V_r} \quad (44)$ $V_r = b Ar_o \quad (45)$	$b$ : mean rooting depth (mm) $\alpha'$ : mean rainfall per event during growing season (mm/event) $\lambda_p$ : frequency of rainfall event during growing season $n$ : soil porosity $\theta_{FC}$ : volumetric moisture content at field capacity $\theta_{WP}$ : volumetric moisture content at wilting point $ETP$ : total evapotranspiration during growing season (mm) $Ar_o$ : roots cross-sectional area at $z=0$ (cm <sup>2</sup> ) $M_a$ : aboveground vegetation biomass (g) $\rho_r$ : root mass density (g/cm <sup>3</sup> ) $\Omega$ : allometric coefficient 1 $\beta$ : allometric coefficient 2 $Az(z)$ : roots cross-sectional area with depth (cm <sup>2</sup> ) $z$ : soil depth (cm) $RAR(z)$ : root area ratio with depth $Ars$ : rooted soil area (cm <sup>2</sup> ) $r(z)$ : root distribution density function (cm <sup>-1</sup> ) $V_r$ : roots profile volume (cm <sup>3</sup> )	Laio et al. (2006) Preti et al. (2010)	- Roots distribution follows negative exponential function - Steady-state mature vegetation - $Ar_o$ is species-specific - $b$ depends on climatic and pedologic predictors - Water is the limiting resource - Isotropic soil - Belowground biomass estimated with allometric model
Plant-water uptake	$U(z) = Etp \frac{\theta(z) - \theta_{WP}}{\theta_{FC} - \theta_{WP}} r(z) \quad (46)$	$r(z)$ : root distribution density function (cm <sup>-1</sup> ) $Etp$ : potential plant transpiration rate (mm/s) $\theta(z)$ : volumetric moisture content at field capacity $\theta_{FC}$ : volumetric moisture content at wilting point $\theta_{WP}$ : volumetric moisture content at wilting point $\theta(z)$ : volumetric moisture content with soil depth $r(z)$ : root density function	Laio (2006)	- Top-down control - Isotropic soil - Uniform moisture content - Only uptake from the root zone
Pedotransfer functions	$\theta_{FC} = \theta_{33} + (1.238\theta_{33}^2 - 0.374\theta_{33} - 0.015) \quad (47)$ $\theta_{33} = -0.251Ss + 0.195Cl + 0.011OM + 0.006SuOM - 0.027ClOM + 0.452SuCl + 0.299 \quad (48)$ $\theta_{WP} = \theta_{1500} + (0.14\theta_{1500} - 0.02) \quad (48)$ $\theta_{1500} = -0.024Ss + 0.487Cl + 0.006OM + 0.005SuMO - 0.013ClOM + 0.068SuCl + 0.031$	$\theta_{FC}$ : volumetric moisture content at field capacity $\theta_{WP}$ : volumetric moisture content at wilting point $\theta_{33}$ : volumetric moisture content at 33 kPa $\theta_{1500}$ : volumetric moisture content at 1500 kPa $Ss$ : sand content $Cl$ : clay content $OM$ : $\phi$ : matric suction of the wetting front $n$ : soil porosity $K_s$ : saturated hydraulic conductivity (m/s) $\theta_{33}$ : volumetric moisture content at 33 kPa $\theta_{1500}$ : volumetric moisture content at 1500 kPa	Rawls & Brakensiek (1985) Saxton & Rawls (2006)	
	$\phi_j = 10^{6.989 - 7.226\theta_1 + 0.05185\theta_1^2 + 3.8047\theta_1 + 0.000344\theta_1^3 - 0.04087\theta_1\phi - 0.000138\theta_1^2\phi - 0.00379\theta_1^3\phi - 0.00079\theta_1^4\phi} \quad (49)$ $K_s = 1930(\theta_s - \theta_{33})^{3-\lambda} \quad (50)$ $\lambda = 1/B \quad (51)$ $B = \frac{\ln(1500) - \ln(33)}{\ln(\theta_{33}) - \ln(\theta_{1500})} \quad (52)$			

**Plant water uptake Sub-model.** Plants uptake water by the roots to attend their physiological needs and it is largely dependent on the atmospheric demand and the plant-available water capacity of the root zone (Rodríguez-Iturbe and Porporato, 2005). Top-down or macroscopic models, based on first principles of energy and mass transfer (Feddes et al., 2002), calculate root water extraction from the plant transpiration rate, spatial distribution of roots and soil water stress. These parameters are relatively easy to estimate (Shukla, 2014) compared to the ones needed in bottom-up or microscopic models. If it is considered that in the long-term all the water that infiltrates into the soil will be eventually lost to transpiration and that roots just uptake water from the root zone, a simple model can be derived from the water mass balance in the soil. Here we adopted the top-down approach

suggested by Laio (2006) (Eq. 46) that requires knowledge of the transpiration rate, estimated in 2.3.4, the soil water stress, dependant on the degree of saturation and the plant-available water capacity, and the root density distribution, estimated through 2.3.5.

### **Case scenario**

A heavy rainfall episode (i.e. 7.2 mm/h for 24 hours, reflecting the total rainfall in a week concentrated in one event) was considered over a 2 m deep (i.e. shallow soil; Lu and Godt, 2008), 1 m<sup>2</sup>, sandy-clay, 45° slope with two mature plant species of different biomass and root tensile strength – Oak tree (*Quercus pyrenaica* Willd.) and Spanish broom (*Spartium junceum* L.) – followed by a drying event for a normal winter day in temperate climate, when landslides are most likely to occur. The initial moisture conditions of the isotropic soil profile were considered to be uniformly distributed and at field capacity. It was assumed that vegetation was active and that their root systems were fully developed. The vegetated slope was compared with a bare slope in terms of stability.

The climatic conditions for predicting the root profiles were estimated from the meteorological time series for Catterline, Scotland, UK (56° 53' 00" N- 2° 12' 00" W), recorded between November 2011 and April 2014 (voor de Poorte, 2014). Rainfall interception was assumed as for a dormant deciduous broadleaf temperate forest (Deguchi et al., 2006) and equal for both vegetation species. Values reported in the literature were used as input parameters (Table 5) to proceed with the model runs.

### **Sensitivity and statistical analysis**

The sensitivity of the independent model parameters was assessed with the One-factor-at-a-time (i.e. OAT; Daniel, 1973) approach. The 11 model variables (i.e.  $S_e$ ,  $C_R$ ,  $\sigma^s$ ,  $i$ ,  $q$ ,  $z_f$ ,  $q_{perc}$ ,  $z_{perc}$ ,  $Eu$ ,  $Az$ ,  $U$ ) were excluded from the analysis and considered as sensitive. 61 model runs were performed after changing the parameter's base value by -20 % and + 20 %, respectively, to account for natural variability. The parameter change that generated the greatest output variation was kept for estimating the sensitivity index (i.e. SI; Eq. 53; Félix & Xanthoulis, 2005) and the percentage of variation (i.e. PV; Eq.54; Félix & Xanthoulis, 2005).

The model output was assessed in terms of the winsorized mean (Wilcox & Keselman, 2003) trimmed at 20 % of the FoS (Eq. 1; after Lu & Godt, 2008)

In addition, a Kruskal-Wallis test was carried out between the winsorized model outputs of the base run at the 95 and 99 % confidence intervals to detect statistical differences between the three considered treatments (i.e. Oak tree, Spanish broom, Bare soil).

**Table 5. Model input parameters and source.**

<b>Symbol</b>	<b>Parameter</b>	<b>Value</b>	<b>Source</b>	<b>Remarks</b>
$P$	Rainfall intensity (mm/h)	7.20	Assumed	See 2.4
$a_1$	Throughfall slope coefficient	0.86	Deguchi et al. (2006)	
$b_1$	Throughfall intercept coefficient	1.06	Deguchi et al. (2006)	
$a_2$	Stemflow slope coefficient	0.06	Deguchi et al. (2006)	
$b_2$	Stemflow intercept coefficient	0.28	Deguchi et al. (2006)	
$k$	Extinction coefficient	0.75	van Dijk & Bruijnzeel (2001)	
$LAI$	Leaf area index Oak	3.48	Deguchi et al. (2006)	
$LAI$	Leaf area index Spanish broom	1.8	Hall (1985)	
$t_r$	Rainfall duration (h)	24	Assumed	See 2.4
$n$	Soil porosity	0.27	Assumed	
$S_a$	Sand content	0.65	Estimated	BS1377:1990
$Cl$	Clay content	0.02	Estimated	BS1377:1990
$OM$	Organic matter content	0.02	Assumed	
$\alpha'$	Mean rainfall intensity/event (mm/event)	0.30	Estimated	See 2.4
$\lambda_o$	Frequency of rainfall	0.55	Estimated	See 2.4
$ETP$	Total ETP per growing season (cm)	42.00	Estimated	See 2.4
$\rho_{roots}$	Roots mass density (g/cm <sup>3</sup> )	0.80	American Chemical Society (2011)	
$\vartheta$	Allometric coefficient 1 Oak	4.55	Cheng & Niklas (2007)	
$\Omega$	Allometric coefficient 2 Oak	0.88	Cheng & Niklas (2007)	
$\vartheta$	Allometric coefficient 1 Spanish broom	3.64	Preti et al. (2010)	
$\Omega$	Allometric coefficient 2 Spanish broom	1.04	Preti et al. (2010)	
$M_a$	Aboveground biomass Oak (g/m <sup>2</sup> )	6140.00	Nunes et al. (2010)	
$M_a$	Aboveground biomass Spanish broom (g/m <sup>2</sup> )	33.00	Preti et al. (2010)	
$K'$	Reinforcement correction factor	0.40	Preti et al. (2013)	
$T_r$	Mean root tensile strength Oak (MPa)	8.00	Stokes et al. (2008)	
$T_r$	Mean root tensile strength Spanish broom (MPa)	32.00	Tosi (2007)	
$AP$	Atmospheric pressure (kPa)	98.00	Estimated	See 2.4
$T_k$	Mean air temperature (K)	279.05	Estimated	See 2.4
$a$	Soil albedo	0.24	Scharmer & Greif (2000)	
$a_s$	Amstrong coefficient 1	0.25	Allen et al. (1998)	
$b_s$	Amstrong coefficient 2	0.50	Allen et al. (1998)	
$LAT$	Latitude (°N)	57	-	
$J$	Day of the year	41	-	
$z_w$	Depth weathering zone (m)	0.50	Lu & Godt (2013)	
$\Delta\phi'$	Variation of angle of internal friction	4.00	Lu & Godt (2013)	
$\phi'$	Angle of internal friction (degrees)	40.00	Lu & Godt (2008)	
$n$	Particle size distribution coeff.	4.75	Lu et al. (2010)	
$\alpha$	Inverse air-entry pressure coeff.	0.08	Lu & Godt (2013)	
$\beta$	Slope angle (degrees)	45	Assumed	
$c'$	Soil cohesion (kPa)	0.00	Lu & Godt (2013)	

**Table 6.** Sensitivity analysis equations, parameters and source.

Sub-model	Equations	Parameters	Source
Sensitivity analysis	$SI = \frac{\frac{S_2 - S_1}{S_m}}{\frac{E_2 - E_1}{E_m}} \quad (53)$ $PV = \left  \frac{S_2 - S_1}{S_1} \right  \times 100 \quad (54)$	$S$ : Sensitivity Index $S_1$ : model output at base value $S_2$ : model output at changed value $S_m$ : average between $S_1$ and $S_2$ $E_1$ : model input parameter at base value $E_2$ : model input parameter at changed value $PV$ : Percentage of Variation	Daniel (1973)

## Results and Discussion

The model output parameters are shown in Table 7.

Symbol	Parameter	Value	Table 7 Model output parameters.
$\theta_{ic}$	Field capacity	0.1	
$\theta_{wp}$	Wilting point	0.01	
$K_s$	Saturated hydraulic conductivity (m/s)	$2.78 \times 10^{-06}$	
$i$	Rainfall Interception (mm)	19.48	
$P_N$	Net rainfall (mm)	153.32	
$\phi_{wf}$	Wetting front head (mm)	2.6	
$F(t_r)$	Cummulative infiltration (mm)	151.77	
$Z_{wf}$	Depth wetting front (mm)	891.19	
$q$	Infiltration rate (m/s)	$1.77 \times 10^{-06}$	
$TT_{perc}$	Percolation travel time (h)	21.78	
$q_{perc}$	Percolation rate (m/s)	$1.68 \times 10^{-06}$	
$Z_{perc}$	Percolation travel distance (mm)	138.96	
$b$	Average rooting depth (mm)	103.86	
$Ar_{o}(0)$	Root area at z=0 Oak (cm <sup>2</sup> )	773.42	
$Ar_{s}(0)$	Root area at z=0 Sp.Broom (cm <sup>2</sup> )	1.01	
$V_r$	Roots volume Oak (cm <sup>3</sup> )	8033.17	
$V_r$	Roots volume Sp.Broom (cm <sup>3</sup> )	10.49	
$M_r$	Belowground biomass Oak (g/m <sup>2</sup> )	6426.54	
$M_r$	Belowground biomass Sp.Broom (g/m <sup>2</sup> )	8.39	
$Eu$	Potential evapotranspiration rate Oak (m/s)	$1.12 \times 10^{-08}$	
$Esp$	Potential evaporation rate from the soil Oak (m/s)	$2.80 \times 10^{-09}$	
$Etp$	Potential transpiration rate Oak (m/s)	$8.46 \times 10^{-09}$	
$Eu$	Potential evapotranspiration rate Sp.Broom (m/s)	$8.07 \times 10^{-09}$	
$Esp$	Potential evaporation rate from the soil Sp.Broom (m/s)	$3.93 \times 10^{-09}$	
$Etp$	Potential transpiration rate Sp.Broom (m/s)	$4.14 \times 10^{-09}$	
$\alpha_x$	Maximum soil depth for evaporation (mm)	113.81	
$W_v$	Vegetation surchage Oak (kPa)	0.12	
$W_v$	Vegetation surchage Sp.Broom (kPa)	$4.00 \times 10^{-04}$	
$\gamma_s^{sat}$	Saturated soil unit weight (kN/m <sup>3</sup> )	21.91	
$\gamma_s^{unsat}$	Unsaturated soil unit weight (kN/m <sup>3</sup> )	20.92	

## Rainfall interception

The model framework estimated an 11.27 % interception by vegetation, leading to a net rainfall of 153 mm and to a decreased steady rainfall rate of 6.37 mm/h. The predicted interception was lower than that reported by Carlyle-Moses & Price (1999) and Deguchi et al. (2006) for the dormant season, suggesting that the model does not overestimate rainfall interception. This may be due to the use of the same

coefficients for the two compared vegetation species, which does not capture their aboveground structural differences (see section 3.3).

### **Infiltration – Percolation; wetting event**

For the considered scenario, the model framework predicted that almost all net rainfall infiltrated vertically into the soil profile at a steady rate of  $1.77 \times 10^{-6}$  m/s without producing ponding and generated a fully saturated wetting front of 891 mm deep. As stated before, one-dimensional vertical flow, as simulated here, occurs in many circumstances in nature (Stokes et al., 2008; Godt et al., 2009; Lu & Godt, 2013), supporting the considered framework.

Percolation occurred in the following 22 hours at a rate of  $1.68 \times 10^{-6}$  m/s and explored 139 mm in the soil profile. As it is shown in the HCF (Fig. 5a) the hydraulic conductivity increases exponentially as the moisture content increases. This would lead to the drainage of water held in the saturated zone but also could trigger the formation of perched saturated zones downwards in the soil profile that might have negative effects on slope stability. This effect may be aggravated by bypass infiltration induced by vegetation roots (Liang et al., 2011).

For the bare soil, infiltration was produced at the gross rainfall rate, penetrating up to 1040 mm in the soil profile and led to a 24 h percolation at a steady rate of  $1.77 \times 10^{-6}$  m/s that explored 376 mm, emphasizing the attenuating effect of the aboveground vegetation on the belowground hydrodynamics.

### **Evapotranspiration; drying event**

Based upon the meteorological conditions for the considered winter day, the model calculated a potential evapotranspiration rate of  $1.12 \times 10^{-8}$  and  $8.07 \times 10^{-9}$  m/s for Oak tree and Spanish broom, respectively. The potential plant transpiration rates were  $8.46 \times 10^{-9}$  m/s for Oak tree and  $4.14 \times 10^{-9}$  m/s for Spanish broom, reflecting differences in the aboveground canopy configuration between the two species (see section 3.1). The estimated total ETP for the considered day was of about 1 mm, which falls in the range suggested by Allen et al. (1998) for cool temperatures.

### **Root distribution profiles**

According to the considered climatological and pedological descriptors (Table 5), the model predicted root profiles of about 500 mm deep (Figs. 4a-4b) with mean rooting depth (i.e.  $b$ ) of 104 mm. This output matches with field observations of uprooted trees in the UK (e.g. Nicoll & Armstrong, 1998; Crow, 2005) and is concurrent with the findings reported in Schenk & Jackson (2002) for a cold-temperate forest. Similarly, studies carried out by the US Forest Service on white oak in Oregon found that the majority of the roots were located within 400 mm from the ground surface. Schwarz et al. (2010) suggested that 90 % of the roots would reinforce the soil in the first 500 mm of soil depth, as predicted here. However, the utilized approach was conceived for water-controlled ecosystems (i.e. arid) and never tested on a temperate climate site presenting more frequent, but less intense, rainfall events (Table 5). In this regard, for its adaptation to a

temperate climate the total evapotranspiration for the growing season was employed as input parameter (Table 5) in the root distribution sub-model (see 2.3.5) for the calculation of  $b$ , instead of using the mean evapotranspiration rate, as it was suggested by Preti et al. (2010); which would lead to infinitely deep root profiles in the considered scenario.

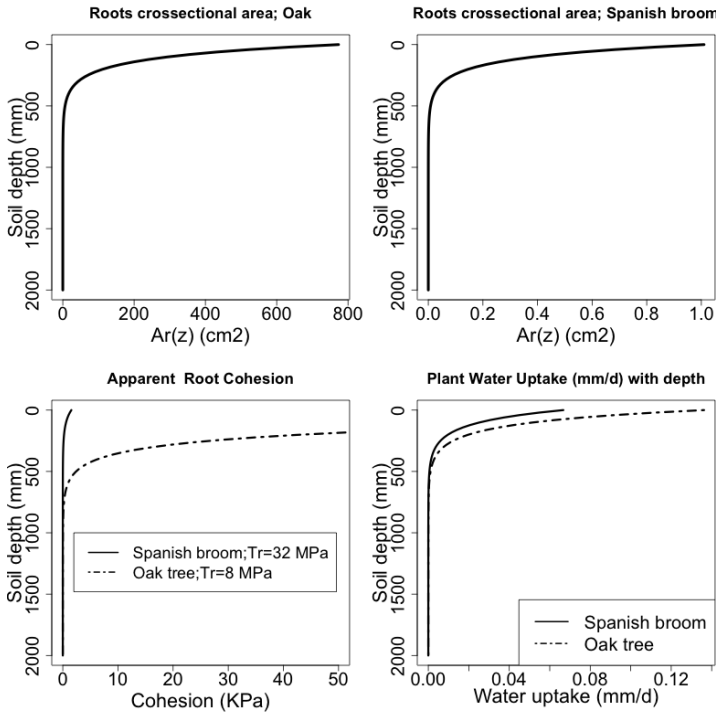


**Figure 4.** *Roots distribution profiles: a) roots cross-sectional area (cm<sup>2</sup>) with depth (mm) for Oak tree; b) roots cross-sectional area (cm<sup>2</sup>) with depth (mm) for Spanish broom; c) Apparent root cohesion (kPa) distribution profiles; Tr: average root tensile strength (MPa); d) Plant water uptake rate (mm/d) distribution profiles.*

### Root mechanical reinforcement

Aboveground biomass differences between the two compared vegetation species (Table 5) led to big differences in terms of the roots cross-sectional area (Figs. 4a-4b), which consequently yielded consistent differences in the RAR (Table 8). These differences were present upon the estimation of the additional root cohesion ( $c_R$ ) and hence, Oak tree presented significantly higher apparent cohesion (Fig. 4c; Table 8) than Spanish broom despite being assigned a four times lower mean root tensile strength. It must be borne in mind that only small roots were considered to compute  $c_R$ , since big roots only contribute to structural anchorage (Mickovski et al., 2009).

**Table 8.** Roots additional cohesion ( $c_R$ ) and root area ratio (RAR) with soil depth. a) model output for Oak tree b) model output for Spanish broom c) laboratory measured values for Willow (Mickovski et al., 2009) d) field measured values for Spanish broom (Tosi, 2007).

Depth (mm)	$C_R^a$ (kPa)	RAR <sup>a</sup>	$C_R^b$ (kPa)	RAR <sup>b</sup>	$C_R^c$ (kPa)	RAR <sup>c</sup>	$C_R^d$ (kPa)	RAR <sup>d</sup>
100	112	$2.9 \times 10^{-2}$	0.58	$3.82 \times 10^{-5}$	30	$2.47 \times 10^{-3}$	9.2	$5.28 \times 10^{-4}$
300	16.05	$4 \times 10^{-3}$	0.08	$5.46 \times 10^{-6}$	10	$6.69 \times 10^{-4}$	14.4	$7.53 \times 10^{-4}$
400	6.07	$1.5 \times 10^{-4}$	0.03	$2.06 \times 10^{-6}$	8	$4.74 \times 10^{-4}$	-	-
600	0.86	$2.26 \times 10^{-4}$	0.004	$2.95 \times 10^{-7}$	-	-	6.2	$2.89 \times 10^{-4}$

Based on the obtained output, the estimated RAR for Oak tree was within the range of documented values in Gray & Baker (2004) (i.e. 0.13-0.008) and beyond the values reported in Mickovski et al. (2009) for Willows. However, RAR was underestimated for Spanish broom (Tosi, 2007) although the predicted root-cross-sectional area profile matches the one reported by Preti et al., (2010) for a silty-clay soil and plant-available water above 30 %. In reference to  $c_R$ , the values for Oak tree were within the common reported values of roots reinforcement (i.e. 2-20 kPa; e.g. Wu et al., 1979; Ekanayake & Phillips, 2002; Mickovski et al., 2009; Comino et al., 2010; Pollen & Simon, 2010) except for the most shallow value, which would be clearly overestimated. For the case of Spanish broom, once again the additional roots cohesion was underestimated (Tosi, 2007); suggesting that the utilized aboveground biomass input value was too low (i.e. 33 g/m<sup>2</sup>) or possible prediction pitfalls of the present framework for low biomass vegetation species. Anyway, it must be borne in mind that this framework does not consider root architecture, which will differ among species and will yield different degrees of soil reinforcement (Stokes et al., 2009).

### Suction stress

The model framework predicted a sharp increase (i.e. from a negative value) in suction stress within the wetted zone while infiltration was occurring (i.e. wetting event; Fig. 5b), mainly due to the increase in the degree of saturation that leads to a drastic reduction of the matric suction (i.e. development of positive pore-water pressures); as shown in the SWCC (Fig. 5a). Nevertheless, the jump was sharper when full saturation within the wetting front was assumed (Fig. 5b), instead of just considering steady infiltration with nearly-saturated conditions (Fig. 5c). This would be likely to occur in the considered soil type (Godt et al., 2009; Lu & Godt, 2013) and was predicted by the infiltration sub-model. In any case, the simulated infiltration rate would lead to a strong increase in suction stress with respect to hydrostatic conditions, which were considered to occur below the percolation front (i.e. soil depth > 1030 mm); where the minimum suction stress was predicted (i.e. -8 kPa).

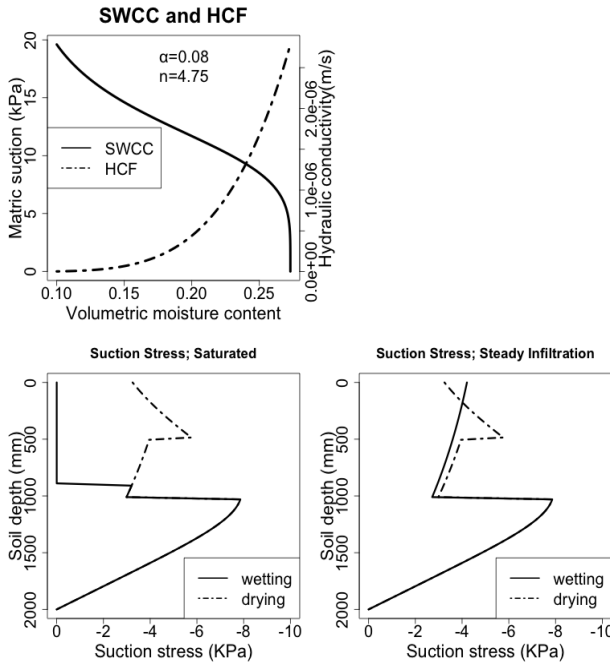


**Figure 5.**

Soil hydrological profiles:  
 a) Soil Water Characteristic Curve (SWCC; van Genuchten (1980) and Hydraulic Conductivity Function (HCF; Brooks and Corey, 1963);  
 $\alpha$ : inverse air-entry pressure parameter ( $\text{kPa}^{-1}$ );  
 $n$ : pore-size distribution parameter;  
 b) Suction stress (kPa) profile for the wetting and drying events assuming full-saturated wetted zone  
 c) Suction stress (kPa) profile for the wetting and drying events assuming steady infiltration rate and nearly-saturated wetted zone.

Contrariwise, similarly to what it has been reported in other studies (e.g. Simon & Collison, 2002, Pollen & Simon, 2010), plant evapotranspiration led to a significant decrease of the suction stress within the root zone (i.e. increase matric suction); reaching a minimum value of about -6 kPa. This outcome indicates that the present framework is not overestimating the effect of vegetation since, for instance, Pollen & Simon (2010) reported an increase of 5 kPa in terms of the matric suction (i.e. ca. -5 kPa of  $\sigma^s$ ). Nonetheless, it is worth noting that negligible differences were found between using the evapotranspiration or the plant-uptake rate for the estimation of the suction stress. Furthermore, although the modelled uptake was higher for Oak tree (i.e. averaged:  $8.82 \times 10^{-11}$  m/s; Fig. 3d) than for Spanish broom (i.e. averaged:  $4.37 \times 10^{-11}$  m/s), due to a higher roots distribution density, only minor differences were found in terms of the suction stress between the two species compared, indicating that further research and improvements of the model framework are needed on this issue.

### Hydro-mechanical effects of vegetation on slope stability

The estimated slope FoSs (Fig. 6a-6c) were strongly influenced by variations in suction stress. Thus, considering the wetted area as fully saturated, failure zones would develop within the saturated zone of the slope (i.e.  $\text{FoS} < 1$ ) as a consequence of the increase in suction stress (i.e. matric suction decrease to 0); supporting that the present model framework captures the hydrological conditions under which landslide episodes occur, as it was validated with a less comprehensive framework by Lu & Godt (2008). Nonetheless, zones in the soil

profile were minimum values of  $\sigma^s$  were predicted presented higher FoS values and therefore more stability.

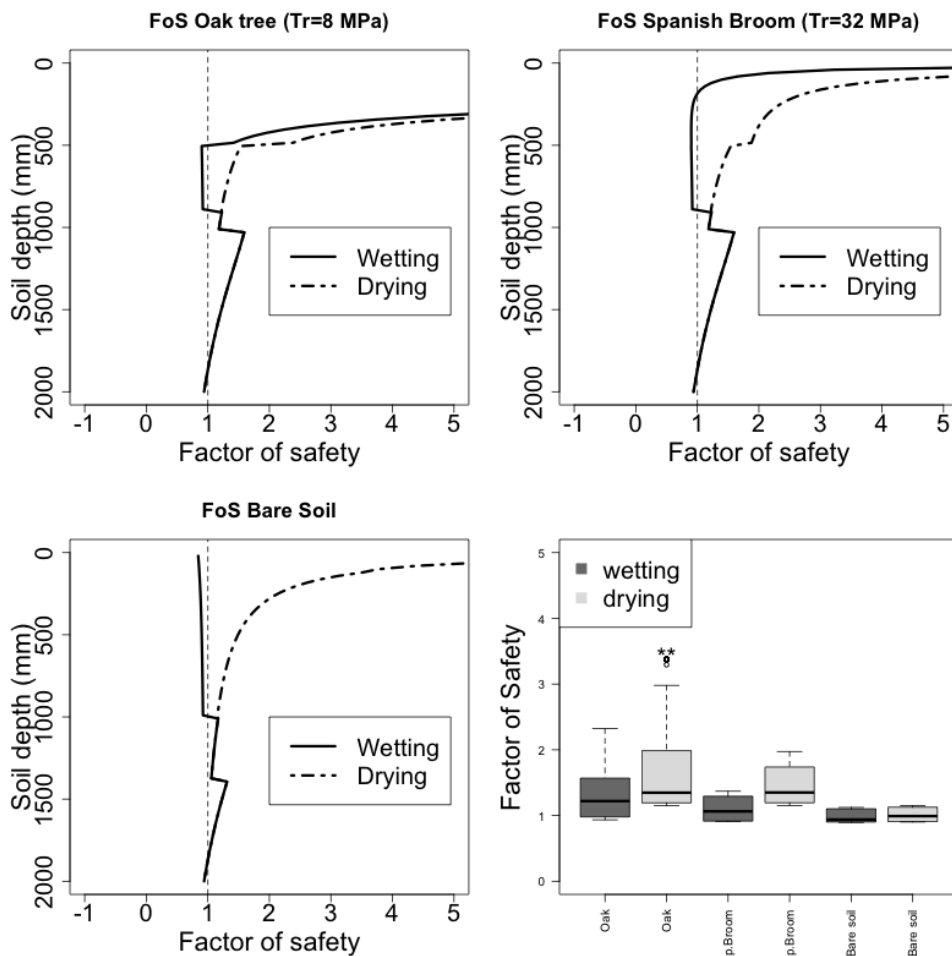


**Figure 6.** Factor of Safety (FoS) profiles for the wetting and drying events for a) Oak tree b) Spanish broom c) Bare soil; c) Boxplot comparing the winsorized FoSs for each of the treatments. \*\*: statistically significant at 99% confidence ( $p < 0.01$ ). Weak zones in the soil profile present a FoS < 1 (i.e. plotline on the left form dashed line). FoS peaks higher than 1 reflect the traveling depth of the wetting and percolating front, respectively.

For the wetting event only the mechanical reinforcement of the vegetation roots would keep the slope stable, stressing the mechanical role of vegetation in slope stability under critical conditions, as it has been reported in other studies (e.g. Ekanayake & Phillips, 2002; Simon & Collison, 2002). As it was expected, the higher biomass species (i.e. Oak tree) would confer significantly ( $\chi^2_{61}=99$ ;  $p < DOI: 10.6092/issn.2281-4485/4535$

0.01) more stability to the slope within the root zone (Fig. 6a), where the higher vegetation surcharge was also producing a positive mechanical effect (e.g. Gray & Megahan, 1981). Nonetheless, Spanish broom also provided a certain degree of mechanical reinforcement (Fig. 6b) despite presenting very low  $c_R$  values (Hubble et al., 2013).

On the other hand, the reduction in suction stress (i.e. towards a more negative value) through plant uptake, or plant transpiration, would significantly increase the slope stability within the root zone (Figs. 5a-5b) even for a winter day if vegetation is active. This emphasises the role of plant transpiration on slope stability as noted in previous studies (e.g. Pollen & Simon, 2010; Simon & Collison, 2002) and highlights the main mechanism by which vegetation produces a positive hydrological contribution to slope stability. Indeed, this effect was even stronger for the lower biomass species (i.e. Spanish broom; Fig. 5b).

It is also worth noting the differences between the factors of safety for the bare soil (Fig. 5c) and the vegetated soil (Figs. 5a-5b), which support the fact that vegetation has a positive effect on slope stability and that the present systematic framework is able to model it.

### Sensitivity analysis

The most sensitive parameter appeared to be the allometric parameter  $\Omega$  (Fig. 7), which relates the above and belowground biomass of the vegetation. This indicates that the present model framework is sensitive to vegetation species and therefore applicable for comparing the effects of different vegetation types on slope stability. The negative sign of  $\Omega$ 's sensitivity index implies that a reduction on the parameter value has a negative effect on the model output (i.e. less biomass-less slope stability). A small change in  $\Omega$  produced a large variation in the model output (i.e. 20 % change induced 120 % change in the output). An accurate estimation of it is needed to improve the predictive capacity of the present framework. Unfortunately, this parameter may be the most expensive parameter to determine since it needs a destructive method for its estimation (Cheng & Niklas, 2007) and will be greatly influenced by the environmental conditions (i.e. climate, soil, nutrient status, etc.) of a particular site (Zianis & Mencuccini, 2004).

Regarding the rest of the parameters, the mechanical properties of the soil, soil cohesion, slope, variation in the angle of internal friction, pore-size distribution and the content of sand, yielded variations on the model output greater than 20 % for the wetting case; indicating specific model outcomes for different soil mechanical properties. Additionally, the average rainfall intensity for the growing season, which in turn shapes the root profile distribution, was also sensitive.

It is worth noting that all parameters were more sensitive for the drying event. This reinforces the relevance of the evapotranspiration process on slope stability and the difficulty to predict it and account for its effects accurately. However, in light of the outcome for the wetting case, the present model framework can be considered as robust since most of the parameters' changes produced minor changes in the output.

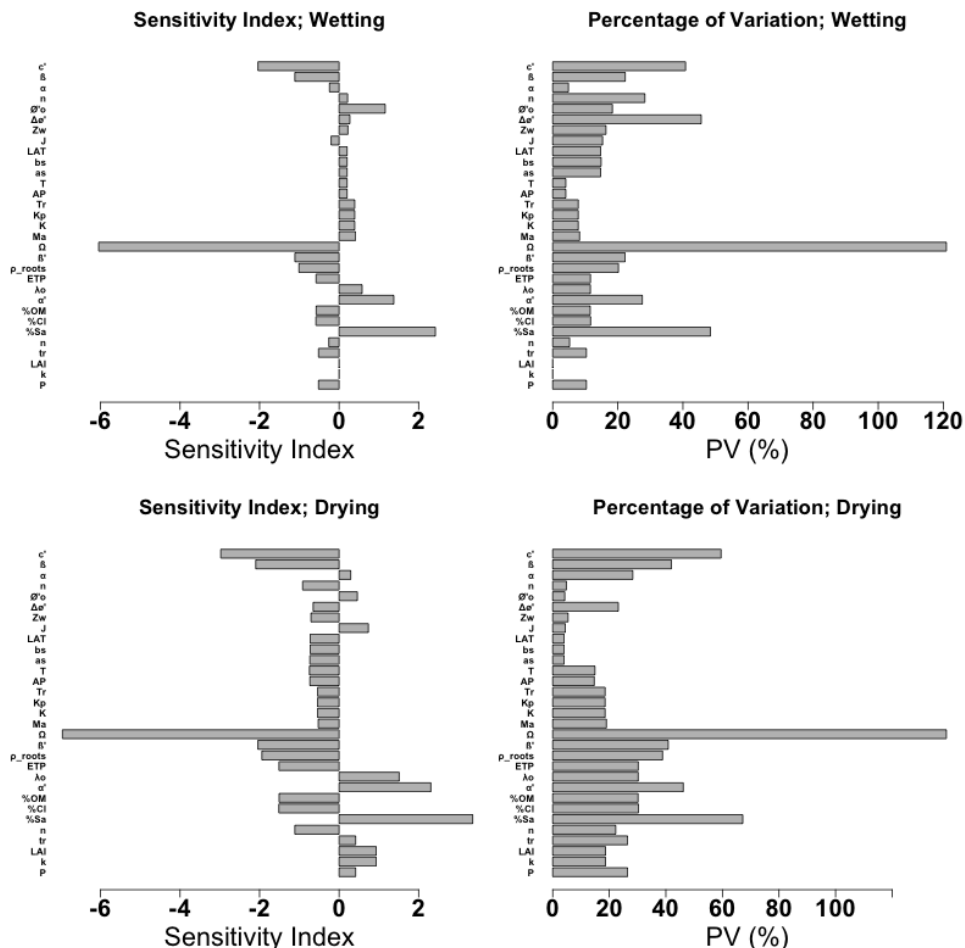


**Figure 7.** Sensitivity analysis output. a) and b) Sensitivity index (SI) for each of the independent model input parameters for the wetting and drying events c) and d) Percentage of variation (PV) for each of the independent model input parameters for the wetting and drying events.

## Conclusions and Outlook

It can be concluded that the proposed model framework simulates the hydro-mechanical effects of vegetation against shallow landslides realistically and in a robust fashion, requiring few, easily measurable and readily available input parameters. Moreover, it is sensitive to vegetation, soil and climate types and it can be easily applied to any site conditions, assisting vegetation selection in soil protection actions and helping to identify vegetation traits necessary for slope stability. Additionally, it permits the detection of weak zones in the soil profile and

allows the assessment of the amount of soil loss and protection. Last but not least, the open source nature of the model's code makes it customizable and freely transferable to land planners, and constitutes a good basis for the extrapolation into larger spatial and temporal scales, or for the inclusion of additional physical processes affected by vegetation and not considered here.

Based on the model output it can be concluded that vegetation has a positive effect on slope stability. Mechanical effects are more relevant when root biomass is higher and under critical hydrological conditions. However, hydrological effects are more relevant when the root biomass is lower. In fact, water abstraction from the root zone appears to be a key process for slope stability even under winter conditions.

The present model framework represents a novel integrated approach; combining for the first time processes on the soil-plant-atmosphere interface in the context of slope stability analysis in the state-of-the-art open source R software. The model is a good tool for the preliminary assessment of the potential effect of vegetation against shallow landslides. However, it is based on limited field data and refinement will be needed together with verification and clarification of the assumptions made.

### **Acknowledgements**

Thanks to Christophe Zreik and Noemi Giupponi for helping with the translations of the abstract.

### **References**

- ALLEN R., PEREIRA L., RAES D., SMITH M. (1998) Crop evapotranspiration-Guidelines for computing crop water requirements. FAO Irrigation and drainage paper 56 .
- ARNOLD J., SRINIVASAN R., MUTTIAH R., WILLIAMS, J. (1998) Large area hydrologic modeling and assessment. Part I: Model development. Journal of the American Water Resources Association, 12:73-89.
- BISHOP A. (1955) The use of the slip circle in the stability analysis of slopes. Géotechnique, 7:7-17.
- BRÈDA N. (2003). Ground-based measurements of leaf area index: a review of methods, instruments and current controversies. Journal of Experimental Botany, 54(392):2403-2417.
- BADC, British Atmospheric Data Centre (2013). Retrieved 6 12, 2014, from <http://badc.nerc.ac.uk>
- BROOKS R., COREY A. (1964) Hydraulic Properties of Porous Media (Vol. 3). Fort Collins, Colorado: Hydrology Papers-Colorado State University.
- CARLYLE-MOSES D., PRICE A. (1999) An evaluation of the Gash model interception model in a Northern hardwood stand. Journal Hydrology, 214:103-110.
- CARTER R., GODFREY, R. G. (1960) Manual of Hydrology: Part 3, Flood-flow techniques: Storage and Flood Routing. Washington: US Government Printing Office.
- CHENG D., NIKLAS K. (2007) Above- and Below-ground Biomass Relationships Across 1534 Forested Communities. Annals of Botany, 99:5-102.

- COMINO E., MARENGO P., ROLLI V. (2010) Root reinforcement effect of different grass species: A comparison between experimental and models results. *Soil & Tillage Research*, 110:60-68.
- CROW P. (2005) *The Influence of Soils and Species on Tree Root Depth*. UK Forestry Commission, Forest Research. Edinburgh: Forestry Commission.
- DANIEL C. (1973) One-at-a-time-plans. *Journal of the American Statistical Association*, 68:353-360.
- DE VOS B., VANDECASTEELE B., DECKERS J., MUYS B. (2005) Capability of Loss-on-Ignition as a Predictor of Total Organic Carbon in Non-Calcareous Forest Soils. *Communications in Soil Science and Plant Analysis*, 36:2899-2921.
- DEGUCHI A., HATTORI S., PARK H. (2006) The influence of seasonal changes in canopy structure on interception loss: Application of the revised Gash model. *Journal of Hydrology*, 318:80-102.
- DUPUY L., FOURCAUD T., LAC P., STOKES A. (2007) A generic 3 D finite element model of tree anchorage integrating soil mechanics and real root system architecture. *Am. J. Bot.*, 94:1506-1514.
- EKANAYAKE J., PHILLIPS C. (1999) A method for stability analysis of vegetated hillslopes: an energy approach. *Canadian Geotechnical Journal*, 36:1172-1184.
- EKANAYAKE J., PHILLIPS C. (2002) Slope stability thresholds for vegetated hillslopes: a composite model. *Canadian Geotechnical Journal*, 39(4):849-862.
- FEDDES R., HOFF H., BRUEN M., DAWSON T., DE ROSNAY P., DIRMEYER P., et al. (2002) Modeling Root Water Uptake in Hydrological and Climate Models. *Bulletin of the American Meteorological Society*, 82(12):2797-2809.
- FÉLIX R., XANTHOULIS D. (2005) Analyse de sensibilité du modèle mathématique "Erosion Productivity Impact Calculator" (EPIC) par l'approche One-Factor-At-A-Time (OAT). *Biotechnol. Agron. Soc. Environ.*, 9(3):179-190.
- GASH J. (1979) An analytical model of rainfall interception by forests. *Quarterly Journal of the Royal Meteorological Society*, 105(443):43-55.
- GODT J., BAUM R., LU N. (2009) Landsliding in partially saturated materials. *Geophysical Research Letters*, 36:L02403.
- GRAY D., BAKER D. (2004) Root-Soil Mechanics and Interactions. *Water Science and Application*, 8:113-123.
- GRAY D., MEHAGAN W. (1981) *Forest Vegetation Removal and Slope Stability in the Idaho Batholith*. US Department of Agriculture Forest Service, Intermountain Forest and Range Experimental Station Research Paper , INT-271, 1-23.
- HEAD K. H. (1980) *Manual of Soil Laboratory Testing*. Boca Raton, FL: CRC Press.
- HEAD K. H., EPPS R. J. (2011) *Manual of Soil Laboratory Testing: Permeability, Shear Strength and Compressibility Tests (Vol. 2)*. Boca Raton, FL: CRC Press.
- HUBBLE T., AIREY D., SEALEY H., DE CARLI E., CLARKE S. (2013) A little cohesion goes a long way: Estimating appropriate values of additional root cohesion for evaluating slope stability in the Eastern Australian highlands. *Ecological Engineering*, 61P:621-632.
- JARVIS N. (1989). A simple empirical model of root water uptake. *Journal of Hydrology*, 107:57-72.
- JORGENSEN S.E., FATH B.D. (2011) *Fundamentals of Ecological Modelling: Application in Environmental Management and Research (4th ed.)*. Amsterdam, The Netherlands: Elsevier.

- LAIO F. (2006) A vertically extended stochastic model of soil moisture in the root zone. *Water Resources Research*, 42:W02406.
- LAIO F., D'ODORICO P., RIDOLFI L. (2006) An analytical model to relate the vertical root distribution to climate and soil properties. *Geophysical Research Letters*, 33:L18401.
- LIANG W., KOSUGI K., MIZUYAMA T. (2011) Soil water dynamics around a tree on a hillslope with or without rainwater supplied by stemflow. *Water Resources Research*, 47:W02541.
- LIM T., RAHARDJO H., CHANG M., FREDLUND D. (1996) Effect of rainfall on matric suctions in a residual slope. *Can. Geotech J.*, 33(4):618-628.
- LU, N., GRIFFITHS, D. (2004). Profiles of Steady-State Suction Stress in Unsaturated Soils. *J. Geotech. Geoenviron. Eng.*, 130(10):1063-1076.
- LU N., LIKOS W. (2004). *Unsaturated Soil Mechanics*. Hoboken, New Jersey: John Wiley & Sons.
- LU N., GODT J. (2008) Infinite slope stability under steady unsaturated seepage conditions. *Water Resources Research*, 44:W11404.
- LU N., GODT J., WU D. (2010) A closed-form equation for effective stress in unsaturated soil. *Water Resources Research*, 46(5):1-14.
- LU N., GODT J. (2013) *Hillslope Hydrology and Stability*. New York: Cambridge University Press.
- MAO Z., BOURRIER F., STOKESA., FOURCAUD T. (2014) Three-dimensional modelling of slope stability in heterogeneous montane forest ecosystems. *Ecological Modelling*, 273:11-22.
- MEIN R., LARSON C. (1973) Modeling Infiltration during a Steady Rain. *Water Resources Research*, 9(2):384-394.
- MICKOVSKI S., VAN BEEK L., SALIN F. (2005) Uprooting resistance of vetiver grass (*Vetiveriza zizoides*). *Plant and Soil*, 278(1-2):33-41.
- MICKOVSKI S.B., HALLETT P.D., BENGOUGH A.G., BRANSBY M.F., DAVIES M.C.R., SONNENBERG R. (2008) The effect of willow roots on the shear strength of soil. In *Advances in GeoEcology 39: The Soils of Tomorrow*. Proceedings of the 5th International Congress of the European Society for Soil Conservation, Palermo, Italy, 25–30 June 2007. Edited by C. Dazzi and E. Constantini. Catena Verlag GmbH, Reiskirchen, Germany. pp. 247–262.
- MICKOVSKI S., HALLET P., BRANSBY M., DAVIS M., SONNENBERG R., BENGOUGH A. (2009) Mechanical reinforcement of soil by willow roots: impacts of root properties and root failure mechanism. *Soil Sci. American Society of Agronomy*, 73(4):1276-1285.
- MINISTERIUM FÜR ENERGIEWENDE, L. U. (n.d.). *Landwirtschafts- und Umweltatlas*. Retrieved 6 12, 2014, from <http://umweltdaten.landsh.de>
- MONTEITH J. (1965) Evaporation and Environment. In G. Fogg, *The State and Movement of Water in Living Organisms* (pp. 205-234). New York: Academic Press.
- MUZYLO A., LLORENS P., VALENTE F., KEIZER J., DOMINGO F., GASH J. (2009) A review of rainfall interception modelling. *Journal of Hydrology*, 370(1):191-206.
- NEITSCH, S., ARNOLD, J., KINIRY, J., & WILLIAMS, J. (2011). *Soil and Water Assessment Tool; Theoretical Documentation*. Texas: Water Resources Institute Technical Report No 406.
- NICOLL, B., & ARMSTRONG, A. (1998). Development of Prunus Root Systems in a City Street: Pavement Damage and Root Architecture. *The International Journal of Urban Forestry*, 22 (3), 259-270.

- NORRIS, J., STOKES, A., MICKOVSKI, S., CAMERAAT, E., VAN BEEK, R., NICOLL, B., et Al. (2008). Slope Stability and Erosion Control: Ecotechnological Solutions . Doordrecht, The Netherlands: Springer.
- PITMAN J. (1989). Rainfall interception by bracken in open habitats-relations between leaf area, canopy storage and drainage rate. *Journal of Hydrology* , 105, 317-334.
- POLLEN-BANKHEAD N., SIMON A. (2010) Hydrologic and hydraulic effects of riparian root networks on streambank stability: Is mechanical root-reinforcement the whole story? *Geomorphology*, 116:353-362.
- PRETI F. (2013) Forest protection and protection forest: Tree root degradation over hydrological shallow landslides triggering. *Ecological Engineering*, 61P:633-645.
- PRETI F., DANI A., LAIO F. (2010). Root profile assessment by means of hydrological, pedological and aboveground vegetation information for bio-engineering purposes. *Ecological Engineering*, 36:305-316.
- PRIESTLEY, C., & TAYLOR, R. (1972). On the Assessment of Surface Heat Flux and Evaporation Using Large-Scale Parameters. *Monthly Weather Review*, 100(2):81-92.
- RAHARDJO H., LEE T.T., LEONG E.C., REZAUR R.B. (2005) Response of a residual soil slope to rainfall. *Canadian Geotechnical Journal* , 42:340-351.
- RAWLS W., BRAKENSIEK D. (1985) Prediction of soil water properties for hydrologic modeling . In E. Jones, & T. Ward, *Watershed management in the 80's* (pp. 293-299). New York, N.Y.: ASCE.
- RAWLS W., STONE J., BRAKENSIEK D. (1989) Infiltration. In L. Lane, & M. Nearing, *USDA-Water Erosion Prediction Project: Hillslope profile model documentation* (Vol. 2, pp. 68-79). West Lafayette, Indiana: USDA-ARS National Soil Erosion Research Laboratory.
- REYNOLDS W. D., ELRICK D. E. (1990) Poned Infiltration From a Single Ring: I, Analysis of Steady Flow. *Soil Sci. Soc. Am. J.*, 54:1233-1241.
- RODRÍGUEZ-ITURBE I., PORPORATO A. (2004) *Ecohydrology of Water-Controlled Ecosystems*. New York, US: Cambridge University Press.
- RUTTER A., KERSHAW K., ROBINS P., MORTON A. (1971) A predictive model of rainfall interception in forests I. Derivation of the model from observations in a plantation of Corsican pine. *Agricultural Meteorology*, 9:367-384.
- SAVABI M.R., NICKS A.D., WILLIAMS J.R., RAWLS W.J. (1989) Water balance and percolation. Ch. 7 In (L.J. Lane and M.A. Nearing, eds.): *USDA - Water Erosion Prediction Project: Hillslope Profile Model Documentation*. NSERL Report No. 2. USDA-ARS National Soil Erosion Research Laboratory, West Lafayette, Indiana.
- SAXTON K., RAWLS W. (2006) Soil Water Characteristic Estimates by Texture and Organic Matter for Hydrologic Solutions. *Soil Sci. Soc. Am. J.*, 70:1569-1578.
- SCHENK H., JACKSON R. (2002) The global biogeography of roots. *Ecological Monographs*, 72(3):311-328.
- SCHWARZ M., COHEN D., OR D. (2010) Root-soil mechanical interactions during pullout and failure of root bundles. *Journal of Geophysical Research*, 115(F4):1-15.
- SHUKLA M. (2014) *Soil Physics: An Introduction*. Boca Raton, Florida: CRC Press.
- SIMON A., COLLISON J. (2002) Quantifying the mechanical and hydrological effects of riparian vegetation on streambank stability. *Earth Surface Processes and Landforms*, 27(5):527-546.
- STOKES A., ATGER C., BENGOUGH A., FOURCAUD T., SIDLE R. (2009) Desirable plant root traits for protecting natural and engineered slopes against landslides. *Plant Soil*, 324:1-30.

- STOKES A., DOUGLAS G., FOURCAUD T., GIADROSSICH F., GILLIES C., HUBBLE T., et Al. (2014) Ecological mitigation of hillslope instability: ten key issues facing researchers and practitioners. *Plant Soil*, 377:1-23.
- STOKES A., NORRIS J., VAN BEEK L., BOGAARD T., CAMMERAAT E., MICKOVSKI S., et Al. (2008) How vegetation reinforces soil on slopes. In J. Norris, A. Stokes, S. Mickovski, E. Cammeraat, R. Van Beek, B. Nicoll, et Al., *Slope Stability and Erosion Control: Ecotechnological Solutions* (pp. 65-116). Dordrecht, The Netherlands: Springer.
- TEAM, R. C. (2012) *The R Foundation for Statistical Software*. Retrieved from <http://www.R-project.org>
- TOSI M. (2007) Root tensile strength relationships and their slope stability implications of three shrub species in the Northern Apennines (Italy). *Geomorphology*, 87, 268-283.
- UK Met Office (2014) UKCP09: *Gridded observation data sets*. Retrieved 12 6, 2014, from <http://metoffice.gov.uk/climatechange/science/monitoring/ukcp09/>
- UNEP, United Nations Environment Programme (2014) Environmental Data Explorer. Retrieved 6 12, 2014, from <http://geodata.grid.unep.ch/>
- US Forest Service (2014) Retrieved 5 13, 2014 from Genetic and Silvicultural Foundations for Management-Oak Studies: <http://www.fs.fed.us/pnw/olympia/silv/oak-studies/oak-roots.shtml>
- VAN DIJK A., BRUIJNZEEL L. (2001) Modelling rainfall interception by vegetation of variable density using an adapted analytical model. Part 1. Model description. *Journal of Hydrology*, 247:230-238.
- VAN GENUCHTEN M. (1980) A Closed-form Equation for Predicting Hydraulic Conductivity of Unsaturated Soils. *Soil Sci. Soc. Am. J.*, 44.:892-898.
- VOOR DE POORTE P. (2014) Meteorological time series of Catterline, Scotland, UK. *Personal communication* .
- WALDRON L. J. (1977) The Shear Resistance of Root-Permeated Homogeneous and Stratified Soil. *Soil Sci. Soc. Am. J.* , 41.
- WALKER L., SHIELS A. (2013) *Landslide Ecology*. Cambridge: Cambridge University Press.
- WILCOX R.R., KESELMAN H. J. (2003) Modern robust data analysis methods: Measures of central tendency. *Psychological Methods* , 8 (3), 254-274.
- WILLIAMS J., OUYANG Y., CHEN J. (1998) *Estimation of infiltration rate in vadose zone: application of selected mathematical models* (Vol. 2). Ada, Oklahoma: US-EPA-National Risk Management Research Laboratory.
- WOLF D., CARSON E., BROWN R. (1972) Leaf Area Index and Specific Leaf Area Determinations. *Jour. of Agron. Educ.* , 1, 24-27.
- WU H., MCKINNELL W., SWANSTON D. (1979) Strength of tree roots and landslides on Prince of Wales Island, Alaska. *Canadian Geotechnical Journal*, 16(1):19-33.
- ZIANIS D., MENCUCCINI M. (2004) On simplifying allometric analyses of forest biomass. *Forest Ecology and Management*, 187:311-332.

## **MODÈLE INTÉGRÉ DES EFFETS HYDRO-MÉCANIQUES DE LA VÉGÉTATION SUR LA STABILITÉ DE LA PENTE**

### **Résumé**

Les glissements de terrain superficiels sont des événements d'instabilité qui conduisent à une perte dramatique du sol dans les zones en pente et sont souvent déclenchés par des épisodes de précipitations intenses. La végétation peut réduire le risque de rupture de talus à travers différents mécanismes hydro-mécaniques qui ont lieu à l'interface sol-plante-atmosphère. Cependant, certains de ces mécanismes, tels les hydrologiques, sont toujours peu compris ou quantifiés. En outre, la plupart des modèles actuels n'ont pas une approche globale, exigent une quantité importante de paramètres d'entrée ou sont difficilement transférables à d'autres utilisateurs.

Dans cet article, un modèle intégré, robuste et reproductible est proposé et évalué dans le but d'estimer les effets hydro-mécaniques des différents types de végétation sur la stabilité de la pente à l'aide de paramètres d'entrée facilement mesurables et quantifiables. Le résultat montre que le modèle d'évaluation est capable de simuler les effets hydro-mécaniques de la végétation d'une manière réaliste et qu'il peut être facilement appliqué à tous les types de végétation, de sol et de climat. Il démontre également que la végétation a des effets hydro-mécaniques positifs sur la stabilité de la pente, où la biomasse végétale et l'évapotranspiration jouent un rôle important.

**Mots clés:** *stabilité de la pente, végétation, effets hydro-mécaniques, modèle intégré, R*

## **MODELLO INTEGRATO PER GLI EFFETTI IDRO-MECCANICI DELLA VEGETAZIONE SULLA STABILITÀ DI VERSANTE**

### **Riassunto**

Le frane di superficie, sono fenomeni di instabilità che determinano la caduta di terreno su aree in pendenza, spesso causati da episodi di intensa pioggia. La vegetazione può ridurre la probabilità delle frane attraverso meccanismi idro-meccanici che si svolgono nell'interfaccia terreno-pianta-atmosfera. Nonostante il ruolo meccanico della vegetazione sia stato ampiamente riconosciuto, i suoi effetti idrologici sono stati quantificati in modo superficiale. In aggiunta, la maggior parte dei modelli esistenti mancano di un approccio olistico, richiedono parametri che sono difficili da misurare o basati su scopi commerciali, rendendoli difficilmente utilizzabili dai gestori del territorio.

In questo articolo, un modello integrato, robusto e riproducibile è proposto e valutato con lo scopo di individuare gli effetti idro-meccanici che diversi tipo di vegetazione hanno sulla stabilità della pendenza usando parametri facilmente misurabili e quantificabili. L'output dimostra che il modello è capace di simulare in maniera realistica gli effetti idro meccanici di qualsiasi vegetazione e che può essere applicato ad ogni tipo di vegetazione, terreno e clima. Il modello dimostra inoltre che la vegetazione ha effetti idro meccanici positivi sugli smottamenti di terreno, dove la biomassa della pianta e l'evapotraspirazione assumono un ruolo importante.

**Parole chiave:** *stabilità della pendenza, vegetazione, effetti idro-meccanici, modello integrato, R*